

Analytical Model for Magnetic Particle Transport in a Magnetically Biased Microfluidic System

E. P. Furlani

The Institute for Lasers, Photonics, and Biophotonics, University at Buffalo SUNY
432 Natural Science Complex
Buffalo, NY 14260-3000
efurlani@buffalo.edu

ABSTRACT

In this presentation we introduce a passive magnetically biased microsystem for the magnetophoretic control of micro/nanoparticles, and a model for predicting its performance. The microsystem consists of an array of integrated soft-magnetic elements embedded beneath a microfluidic channel. The elements are polarized by a bias field, and produce a nonuniform field distribution that gives rise to a magnetic force on particles as they flow through the microchannel. We use analytical expressions for the dominant magnetic and fluidic forces on the particles, and solve the equations of motion to study particle transport within the microsystem. We show that the microsystem is capable of efficient particle capture, and discuss its use for biomedical applications.

Keywords: magnetophoresis, magnetic microsystem, micro total analysis system, magnetic bioseparation, magnetophoretic microsystem

1 INTRODUCTION

The interest in magnetophoretic microsystems is substantial and growing rapidly due primarily to biomedical applications such as bioseparation where magnetic particles are used to label, manipulate, and immobilize biomaterials such as cells, enzymes, proteins, and DNA [1]. There has been a rapid increase in the applications of magnetically functional microsystems due to advances in microfluidic technology, and the development of functionalized magnetic particles that can selectively label, isolate, and transport a target biomaterial.

Magnetophoretic microsystems are well suited for bioapplications because they enable (i) fast reaction times, (ii) efficient coupling between the applied field and magnetically labeled biomaterial, (iii) the analysis and monitoring of small samples (picoliters), and (iv) the integration of “micro total analysis systems” (μ TAS).

In this presentation we introduce a passive magnetophoretic microsystem, and present a model for analyzing its performance. We also discuss its application to biomedical science. The microsystem consists of an

array of integrated soft-magnetic elements embedded in a nonmagnetic substrate, beneath a microfluidic channel

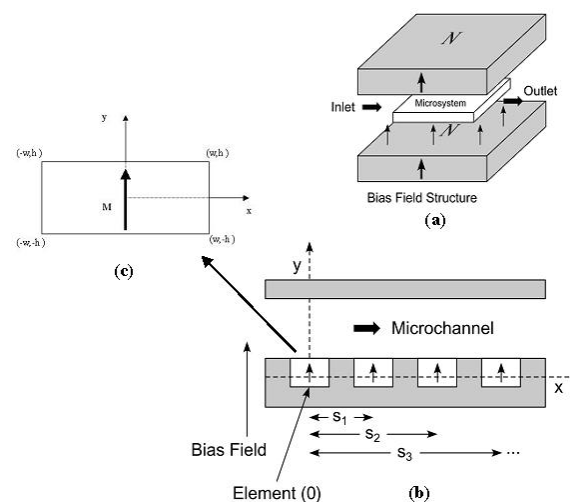


Figure 1: Magnetophoretic microsystem: (a) microsystem and bias magnets, (b) cross sectional view showing embedded magnetic elements and reference frame, and (c) 0'th magnetic element with reference frame.

(Fig. 1). A bias field is used to magnetize the elements, which in turn produce a magnetic force on particles within the microchannel. We model the behavior of the particles using analytical expressions for the dominant magnetic and fluidic forces. Specifically, we apply these expressions to the equations of particle motion, which are solved numerically to study particle transport within the microsystem. The model takes into account key variables including the size and properties of the particles, the bias field, the dimensions of the microchannel, the fluid properties, and the flow velocity. We use it to study particle transport, and our analysis demonstrates that the microsystem is capable of efficient particle capture, which makes it a viable candidate for a variety of bioapplications. The analysis also shows that the particles exhibit an oscillatory motion as they traverse the microsystem, which could be used to characterize fluids at the micro or nanoscale.

2 THEORETICAL MODEL

Particle transport in a magnetophoretic microsystem is governed by various factors including (a) the magnetic force due to all field sources, (b) the fluidic drag force, (c) inertia, (d) gravity, (e) buoyancy, (f) thermal kinetics, (g) particle/fluid interactions (perturbations to the flow field), and (h) interparticle effects such as (i) magnetic dipole interactions, (ii) electric double-layer interactions, and (iii) van der Waals force. For magnetophoretic applications involving submicron particles in dilute suspensions, the magnetic and viscous forces are dominant, and we predict particle motion using Newton's law,

$$m_p \frac{d\mathbf{v}_p}{dt} = \mathbf{F}_m + \mathbf{F}_f, \quad (1)$$

where m_p and \mathbf{v}_p are the mass and velocity of the particle, and \mathbf{F}_m and \mathbf{F}_f are the magnetic and fluidic forces respectively. The inertial term $m_p d\mathbf{v}_p/dt$ is small, but we include it here to obtain greater accuracy during periods of high acceleration. The magnetic force is given by

$$\mathbf{F}_m = \mu_0 V_p (\mathbf{M}_p \bullet \nabla) \mathbf{H}_a, \quad (2)$$

where V_p and \mathbf{M}_p are the volume and magnetization of the particle, and \mathbf{H}_a is the applied magnetic field intensity inside the particle (taken to be at the center of the particle). The fluidic force is based on Stokes' approximation for the drag on a sphere

$$\mathbf{F}_f = -6\pi\eta R_p (\mathbf{v}_p - \mathbf{v}_f), \quad (3)$$

where η and \mathbf{v}_f are the viscosity and the velocity of the fluid, respectively.

This approach does not take into account Brownian motion, which can influence particle capture when the particle diameter D_p is sufficiently small. Gerber et al. [2] have developed the following criterion to estimate this diameter

$$|F| D_p \leq kT, \quad (4)$$

where $|F|$ is the magnitude of the total force acting on the particle, k is Boltzmann's constant, and T is the absolute temperature. For example, for Fe_3O_4 particles in water in a single wire capture mode, the threshold diameter $D_p = kT/|F|$ is 40 nm [2]. For particles with a diameter below this value one solves the following advection-diffusion equation for the particle number density c , rather than the Newtonian equation for the trajectory of a single particle,

$$\frac{\partial c}{\partial t} + \nabla \bullet \mathbf{J} = 0, \quad (5)$$

where $\mathbf{J} = \mathbf{J}_D + \mathbf{J}_F$ is the total flux of particles, which includes a contribution $\mathbf{J}_D = -D\nabla c$ due to diffusion, and a contribution $\mathbf{J}_F = \mathbf{v}c$ due to the action of all external forces.

2.1 Magnetic Force

Analytical expressions for the magnetic force in the microsystem have been previously derived [3]. To determine the magnetic force, we need an expression for the magnetic response of the particles. We use a linear magnetization model with saturation in which

$$\mathbf{M}_p = f(H_a) \mathbf{H}_a, \quad (6)$$

where

$$f(H_a) = \begin{cases} \frac{3(\chi_p - \chi_f)}{(\chi_p - \chi_f) + 3} & H_a < \left(\frac{(\chi_p - \chi_f) + 3}{3(\chi_p - \chi_f)} \right) M_{sp} \\ M_{sp} / H_a & H_a \geq \left(\frac{(\chi_p - \chi_f) + 3}{3(\chi_p - \chi_f)} \right) M_{sp} \end{cases}. \quad (7)$$

M_{sp} is the saturation magnetization of the particle, and χ_p and χ_f are the susceptibilities of the particle and fluid respectively. The field components due to a single magnetic element of width $2w$ and height $2h$ that is centered with respect to the origin in the x - y plane and magnetized to saturation M_{es} (Fig. 1c) are as follows [3], [4]

$$H_{ax}^{(0)}(x, y) = \frac{M_{es}}{4\pi} \left\{ \ln \left[\frac{(x+w)^2 + (y-h)^2}{(x+w)^2 + (y+h)^2} \right] - \ln \left[\frac{(x-w)^2 + (y-h)^2}{(x-w)^2 + (y+h)^2} \right] \right\}, \quad (8)$$

and

$$H_{ay}^{(0)}(x, y) = \frac{M_{es}}{2\pi} \left\{ \tan^{-1} \left[\frac{2h(x+w)}{(x+w)^2 + y^2 - h^2} \right] - \tan^{-1} \left[\frac{2h(x-w)}{(x-w)^2 + y^2 - h^2} \right] \right\}. \quad (9)$$

Let N_e denote the number of elements in the array, and let the first element be centered with respect to the origin in the x - y plane. All other elements are positioned along the x -axis as shown in Fig. 1b. We identify the elements using the index $n = (0, 1, 2, 3, 4, \dots, N_e - 1)$. The field components due to the first element ($n = 0$) are given by Eqs. (8), (9). The n 'th element is centered at $x = s_n$, and its field and force components can be written in terms of the 0'th components as follows:

$$H_{ex}^{(n)}(x, y) = H_{ex}^{(0)}(x - s_n, y) \quad (n = 1, 2, 3, \dots) \quad (10)$$

$$H_{ey}^{(n)}(x, y) = H_{ey}^{(0)}(x - s_n, y).$$

The total field of the array is obtained by summing the contributions from all the elements,

$$H_{ex}(x, y) = \sum_{n=0}^{N_e-1} H_{ex}^{(0)}(x - s_n, y), \quad (11)$$

$$H_{ey}(x, y) = \sum_{n=0}^{N_e-1} H_{ey}^{(0)}(x - s_n, y), \quad (12)$$

The force components are given by [4]

$$\begin{aligned} F_{mx}(x, y) = \mu_0 V_p f(H_a) & \left[\left(\sum_{n=0}^{N_e-1} H_{ex}^{(0)}(x - s_n, y) \right) \right. \\ & \times \left(\sum_{n=0}^{N_e-1} \frac{\partial H_{ex}^{(0)}(x - s_n, y)}{\partial x} \right) \\ & + \left(H_{bias,y} + \sum_{n=0}^{N_e-1} H_{ey}^{(0)}(x - s_n, y) \right) \\ & \left. \times \left(\sum_{n=0}^{N_e-1} \frac{\partial H_{ex}^{(0)}(x - s_n, y)}{\partial y} \right) \right], \end{aligned} \quad (13)$$

and

$$\begin{aligned} F_{my}(x, y) = \mu_0 V_p f(H_a) & \left[\left(\sum_{n=0}^{N_e-1} H_{ex}^{(0)}(x - s_n, y) \right) \right. \\ & \times \left(\sum_{n=0}^{N_e-1} \frac{\partial H_{ey}^{(0)}(x - s_n, y)}{\partial x} \right) \\ & + \left(H_{bias,y} + \sum_{n=0}^{N_e-1} H_{ey}^{(0)}(x - s_n, y) \right) \\ & \left. \times \left(\sum_{n=0}^{N_e-1} \frac{\partial H_{ey}^{(0)}(x - s_n, y)}{\partial y} \right) \right]. \end{aligned} \quad (14)$$

In Eqs. (13) and (14) we have assumed that the bias field is constant and in the y-direction.

2.2 Fluidic Force

The fluidic force is based on Stokes' drag on a sphere. We assume fully developed laminar flow in the microchannel, and use a 2D approximation for the flow velocity profile. The fluidic force is given by

$$\mathbf{F}_{fx} = -6\pi\eta R_{p,hyd} \left[\mathbf{v}_x - \frac{3\bar{v}_f}{2} \left[1 - \left(\frac{y - (h + h_c)}{h_c} \right)^2 \right] \right], \quad (15)$$

and

$$\mathbf{F}_{fy} = -6\pi\eta R_{p,hyd} \mathbf{v}_y, \quad (16)$$

where h and h_c are the half-heights of the magnetic elements and channel, respectively, \bar{v}_f is the average fluid velocity, and $R_{p,hyd}$ is the effective hydrodynamic radius, which can be different than the particle radius R_p if a layer of biomaterial is bound to the surface of the particle [3].

2.3 Equations of Motion

The equations of particle motion through the microsystem can be written in component form by substituting Eqs. (13) - (16) into Eq. (1),

$$\begin{aligned} m \frac{dv_x}{dt} = F_{mx}(x, y) - 6\pi\eta R_{p,hyd} \\ \times \left[\mathbf{v}_x - \frac{3\bar{v}_f}{2} \left[1 - \left(\frac{y - (h + h_c + t_b)}{h_c} \right)^2 \right] \right] \end{aligned} \quad (17)$$

$$m \frac{dv_y}{dt} = F_{my}(x, y) - 6\pi\eta R_{p,hyd} \mathbf{v}_y, \quad (18)$$

$$\mathbf{v}_x(t) = \frac{dx}{dt}, \quad \mathbf{v}_y(t) = \frac{dy}{dt}. \quad (19)$$

We solve these coupled equations using the Runge-Kutta method.

3 APPLICATIONS

The microsystem can be used for numerous bioapplications including bioseparation. We demonstrate this by studying particle transport in it. Specifically, we study the behavior of magnetite (Fe_3O_4) particles in a microsystem with a fluid channel that is 80 μm high, 1 mm wide, and 5 mm long ($h_c = 40 \mu\text{m}$). The fluid is nonmagnetic ($\chi_f = 0$), and has a viscosity and density equal to that of water, $\eta = 0.001 \text{ N}\cdot\text{s}/\text{m}^2$, and $\rho_f = 1000 \text{ kg}/\text{m}^3$. There are 15 permalloy (78% Ni 22% Fe, $M_{es} = 8.6 \times 10^5 \text{ A}/\text{m}$) elements embedded immediately beneath the microchannel [3]. Each element is 80 μm high, and 160 μm wide ($h = 40 \mu\text{m}$, $w = 80 \mu\text{m}$), and they are spaced 80 μm apart (edge to edge). We assume that a bias field of 0.25 T is applied, which is sufficient to saturate the elements.

The Fe_3O_4 particles have the following properties: $R_p = 50 \text{ nm}$, $\rho_p = 5000 \text{ kg}/\text{m}^3$, and $M_{sp} = 4.78 \times 10^5 \text{ A}/\text{m}$. The magnetization function (7) for these particles reduces to

$$f(H_a) = \begin{cases} 3 & H_a < M_{sp}/3 \\ M_{sp}/H_a & H_a \geq M_{sp}/3 \end{cases} \quad (20)$$

We assume that each particle carries surface-bound biomaterial that increases its effective hydrodynamic radius to $R_{p,hyd} = 55$ nm, an increase of 10%. This effective radius is used to compute the fluidic drag force (15)-(16).

We study the behavior of a particle as it moves through the microsystem. We assume that the particle enters the microchannel to the left of the first element at $x(0) = -5w$, and compute its trajectory as a function of its initial height above the magnetized elements: $\Delta y = 4$ μm , 8 μm , ..., 60 μm (i.e., initial heights of $y(0) = 44$ μm , 48 μm , ..., 100 μm). The average fluid velocity is $\bar{v}_f = 5$ mm/s, and the particle enters the channel with this velocity. The predicted trajectories are shown in Fig 2. The analysis indicates that all of the particles that enter the microchannel at a height $\Delta y \leq 60$ μm above the elements will be magnetically attracted to the bottom, where they will be held in place (captured) by the horizontal magnetic force. Notice that the particles exhibit an oscillatory motion as they flow through the channel. This is due to the periodic nature of the magnetic force above the elements, and could potentially be used to characterize the rheology of the transport fluid [3]. A normalized plot of the distribution of captured particles is shown in Fig. 3.

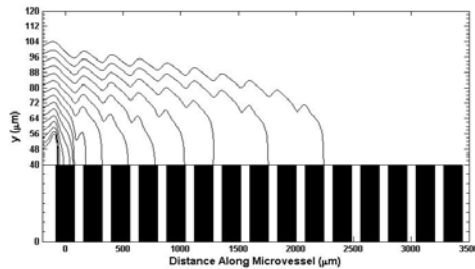


Figure 2: Particle trajectories showing particle capture in the microsystem.

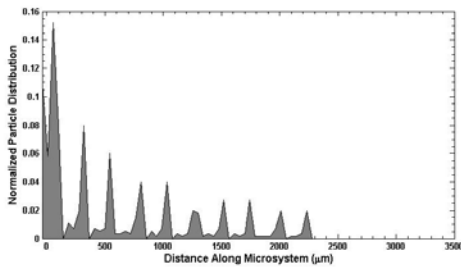


Figure 3: Normalized particle distribution showing variations in particle capture along the microsystem.

The capture time in this microsystem is on the order of minutes, which makes it well-suited for rapid separation of biomaterial from small specimens.

The microsystem also has the potential for use as a blood cell separator [5]. In this mode of operation the flow in the microchannel is aligned with the gravitation force. Deoxygenated red blood cells (RBC) and white blood cells (WBC) (which exhibit paramagnetic and diamagnetic behavior in plasma, respectively) are introduced at the top of the microchannel, and are separated from one another as they flow down through the channel due to the oppositely directed forces that they experience (Fig. 4b).

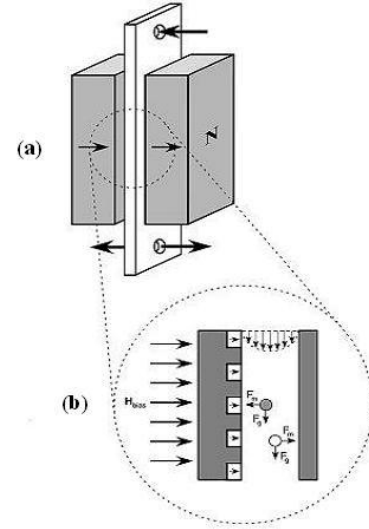


Figure 4: Microsystem for continuous separation of red and white blood cells (RBC and WBC).

4 CONCLUSIONS

We have presented a passive magnetophoretic microsystem, and a model for predicting its performance. The model is analytically-based, and well-suited for parametric design and optimization. The microsystem and model can be applied to the development and optimization of novel devices for bioapplications such as bioseparation.

REFERENCES

- [1] M. A. M. Gijs "Magnetic bead handling on-chip: new opportunities for analytical applications," *Microfluidics and Nanofluidics*, 1(1):22-40, 2004.
- [2] R. Gerber, M. Takayasu, and F. J. Friedlander, "Generalization of HGMS theory: the capture of ultra-fine particles," *IEEE Trans. Magn.* 19 (5), 2115-2117 1983.
- [3] E. P. Furlani, "Analysis of Particle Transport in a Magnetophoretic Microsystem," *J. Appl. Phys.* **99**, 2006.
- [4] E. P. Furlani, *Permanent Magnet and Electromechanical Devices; Materials, Analysis and Applications*, Academic Press, NY, 2001.
- [5] E. P. Furlani, "Magnetophoretic Separation of Blood Cells at the Microscale," *Appl. Phys. Lett.*, under review, 2006.